

# The effective chemical vapour deposition rate of diamond

P. G. PARTRIDGE, M. N. R. ASHFOLD\*, P. W. MAY\*, E. D. NICHOLSON\*  
*Interface Analysis Centre, and \*School of Chemistry, University of Bristol,  
Bristol BS8 1TS, UK*

The effective chemical vapour deposition (CVD) rate of diamond, defined as the total thickness of diamond or as the mass of diamond deposited per unit time, may be increased by orders of magnitude by increasing the substrate area per unit volume. To obtain these high deposition rates, novel substrate designs are proposed that exploit three-dimensional arrays of small diameter wires or fibres. The analysis suggests that the increased diamond output should be achieved with no increase in the net gas flow or power consumption, which could lead to the more economic production of solid diamond shapes and of composites containing continuous or short diamond fibres, or particulate diamond. Estimates for the cost of CVD diamond made by the fibre array technique are compared with reported current and predicted costs for CVD diamond and estimates for the cost of CVD SiC.

## 1. Introduction

It has long been recognised that natural diamond possesses a unique combination of physical, mechanical and chemical properties. There is now increasing evidence that under suitable processing conditions many of these properties can be obtained in diamond produced by chemical vapour deposition (CVD) [1, 2]. Hitherto CVD diamond has been available only in the form of thin films (typically  $< 100 \mu\text{m}$ ) on suitable substrates, and the applications for CVD diamond have been limited to optical coatings or coatings designed to provide wear or abrasion resistance. However, thick-section, large-area, free-standing CVD diamond deposits (300 mm diameter and  $\geq 300 \mu\text{m}$  thick) are now becoming available for the thermal management market [3–5].

Another important development, that could substantially increase the market for CVD diamond, is the production of continuous CVD diamond fibres [1]. These are produced in a hot-filament reactor (HFCVD) [6, 7] by depositing CVD diamond on to metal wire or ceramic fibre cores held near a filament at about  $2000^\circ\text{C}$  in a methane/hydrogen mixture at a pressure of about 30 torr (1 torr = 133.322 Pa) [6]. Deposition on to fibres has also been carried out in a microwave reactor (MWCVD) [8]. Fibre core materials have included metallic wires such as copper, molybdenum, tungsten and titanium [6, 7] and a variety of non-metallic fibres [9–11]. The latter have been either the very small  $\sim 10\text{--}20 \mu\text{m}$  diameter fibres produced in multifilament tows, such as Hi-Nicalon (Si–C–O, Nippon Carbon), Tyranno (Si–C–O–Ti, Ube) and Nextel ( $\text{Al}_2\text{O}_3\text{--SiO}_2\text{--B}_2\text{O}_3$ , 3M) [12] or the larger  $100\text{--}150 \mu\text{m}$  diameter commercial SiC monofilaments [6, 8] and vapour-grown carbon fibres [13, 14]. Under the correct diamond deposition conditions

in the gas phase, all suitable substrate surfaces, separated from each other by distances greater than the mean free path for the active gas radicals, will be coated simultaneously with a diamond film.

The CVD diamond fibres may be used to reinforce polymer, metal or ceramic matrix composites. They offer the engineer, for the first time, the possibility of exploiting the properties of diamond on a large scale in engineering components and structures [1, 15]. These are early days in the development of diamond fibres and many aspects of the diamond deposition process need further research. Of these one of the most important is the diamond deposition rate [1]. A very slow deposition rate of  $R \sim 0.5\text{--}1 \mu\text{m h}^{-1}$  is generally found necessary for high-quality diamond produced in hot-filament and microwave reactors, compared with, for example, deposition rates orders of magnitude greater for CVD of boron and SiC fibres [9]. Higher deposition rates lead to greater concentrations of non-diamond polymorphs and a rapid decrease in the elastic modulus of diamond. The slow deposition rate is largely responsible for the high predicted cost of CVD diamond [1], and may at present be limiting both the market size and the diversity of the applications for CVD diamond. Major advances are now being made in high-power microwave plasma CVD reactors, with reported increases in deposition rates of two orders of magnitude over the last four years [4].

In this paper it is shown that higher effective diamond deposition rates may be obtained by novel substrate designs that make use of the high surface area of wires or fibres. Together with parallel developments in CVD reactors, these designs may enable the more economic manufacture of diamond composites.

## 2. Diamond deposition rate

The diamond deposition rate on free-standing substrates with flat and cylindrical surfaces is shown schematically in Fig. 1. If  $\delta x = x_1$  is the increase in diamond deposit thickness measured normal to the substrate surface after a time  $t$  (Fig. 1a), the conventional deposition rate is given by  $R = x_1/t$ .

It is sometimes convenient to consider an effective diamond deposition rate,  $R_{\text{eff}}$ , defined as the rate of increase in the total thickness of diamond in a particular direction. In the  $Y$  directions in Fig. 1,  $R_{\text{eff}}$  is  $x_1/t$  for one flat surface (Fig. 1a),  $2x_1/t$  for two flat surfaces (Fig. 1b) and  $2x_1/t$  along the diametral direction of a cylindrical shape (Fig. 1c).

The volume (or mass) of diamond deposited per unit time is also used as a measure of the deposition

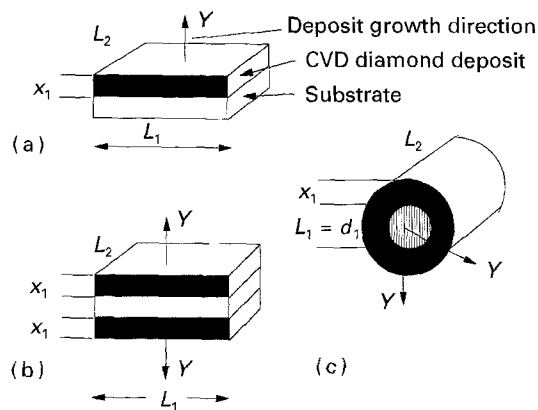


Figure 1 Schematic diagram of three specimens with projected areas ( $L_1 \times L_2$ ) after diamond deposition: (a) a single flat substrate surface, (b) two flat substrate surfaces, and (c) cylindrical surface.

rate [4]. The specimens shown in Fig. 1 have the same projected areas,  $L_1 \times L_2$ , and if  $N$  is the number of specimens coated simultaneously, the volume of diamond deposited is:

on multiple single flat surfaces

$$\text{(Fig. 1a)} \quad V_1 = x_1 L_1 L_2 N \quad (1)$$

on multiple double flat surfaces

$$\text{(Fig. 1b)} \quad V_2 = 2x_1 L_1 L_2 N \quad (2)$$

on multiple cylindrical surfaces

$$\text{(Fig. 1c)} \quad V_3 = \pi(L_1 x_1 + x_1^2) L_2 N \quad (3)$$

For typical values of  $x_1/L_1$  of 0.10–10, the corresponding mass or volume ratios are  $V_1:V_2:V_3 = 1:2:3.5\text{--}35$ . Thus, in practice, the mass of diamond deposited per unit time is proportional to the total substrate area and may be an order of magnitude greater for cylindrical surfaces than for a single flat surface.

## 3. Effective diamond deposition rate on a planar surface

The nucleation of diamond films is heterogeneous on most materials [16, 17]. Then the effective deposition rate,  $R_{\text{eff}}$ , can differ significantly in the principal directions normal ( $X$ ) and parallel ( $Y$ ) to the substrate. An example of preferential diamond nucleation and columnar grain growth along surface scratches and complete absence of nucleation on areas between the scratches is shown in Fig. 2 [18] and schematically in Fig. 3a. Complete coverage of the surface subsequently occurs by deposition on the faces normal to both the directions  $Y$  and  $X$  until the areas between

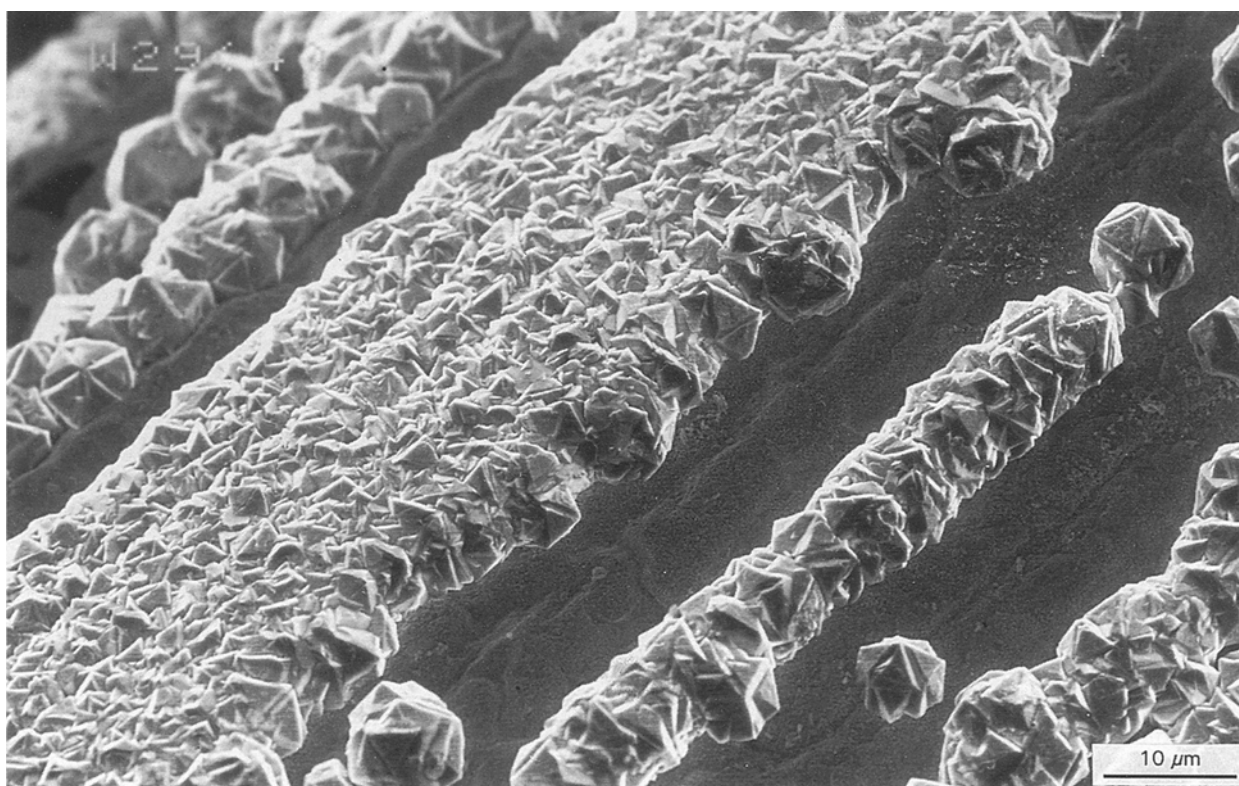


Figure 2 Scanning electron micrograph of heterogeneous diamond nucleation on a tungsten wire surface [18].

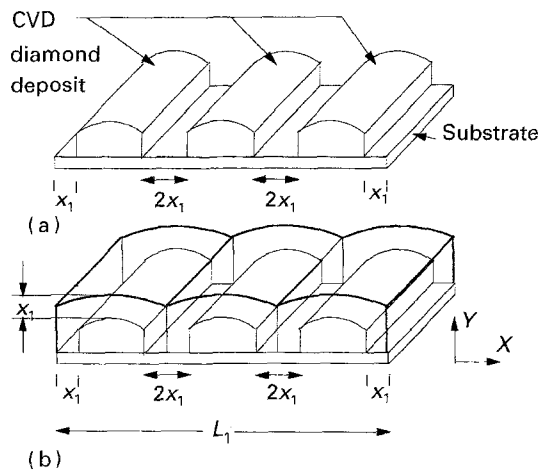


Figure 3 Schematic diagram of heterogeneous diamond nucleation and growth: (a) initial nucleation, and (b) continuous diamond coating.

the scratches are completely coated with diamond, as shown in Fig. 3b. This explains why deposits that initially nucleate only on scratches to produce thick bands of diamond (Fig. 2), eventually produce continuous and uniformly thick films and not films with a stepped surface [18].

This method of covering a surface illustrates the effect of multiple surfaces in increasing the effective diamond deposition rate. Consider the total increase in diamond thickness and the effective deposition rates,  $R_{\text{eff}}$ , in the principal directions  $X$  and  $Y$  in Fig. 3b. In the  $Y$  direction the corresponding values are  $x_1$  and  $R_{\text{eff}} = x_1/t$ . In the  $X$  direction over a distance  $L_1$  which includes deposition on six surfaces, the values are  $6x_1$  and  $R_{\text{eff}} = 6x_1/t = 6R$ . In this example, for the same deposition time, more diamond is deposited in the  $X$  direction than in the  $Y$  direction. In homogeneous diamond nucleation, surface coverage is virtually instantaneous. In this example of heterogeneous nucleation, the time for surface coverage depends primarily on the number of nuclei,  $N$ , with surfaces normal to the  $X$  direction. A total thickness,  $Nx_1$ , of diamond is deposited at an effective diamond deposition rate of  $R_{\text{eff}} = Nx_1/t = NR$  until the surface is completely covered. This high effective diamond deposition rate can be exploited by deposition on to wires and fibres.

#### 4. Effective diamond deposition rate on wires or fibres

Consider uniform diamond deposition on to a planar parallel array of  $N$  straight cylindrical wires of diameter  $d_1$  with a distance,  $s$ , between the wires (Fig. 4a). After a time,  $t$ , the total diamond deposit thickness in the directions  $Y$  and  $X$  is  $2x_1$  and  $2Nx_1$  respectively (Fig. 4a,b), to give the corresponding effective diamond growth rates for these directions of  $R_{\text{eff}} = 2R$  and  $R_{\text{eff}} = 2NR$ . The spaces between the wires will be filled and a free-standing sheet will be formed (Fig. 4b) when  $x_1 = s/2$ . The critical time,  $t_c$ , to fill the space between the wires is dictated by the spacing between the wires because  $t_c = 2x_1/R = s/R$ . Further

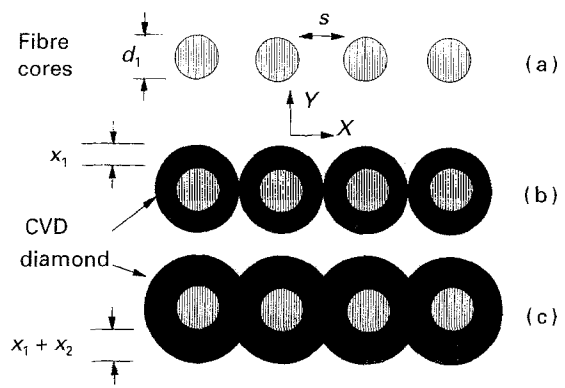


Figure 4 Schematic diagram of diamond deposition on cylindrical cores: (a) section through parallel rows of cores, (b) after diamond coating for time  $t = t_c$  to produce coating of thickness  $x_1$ , and (c) after diamond coating for time  $t > t_c$  to produce coating of thickness  $x_1 + x_2$ .

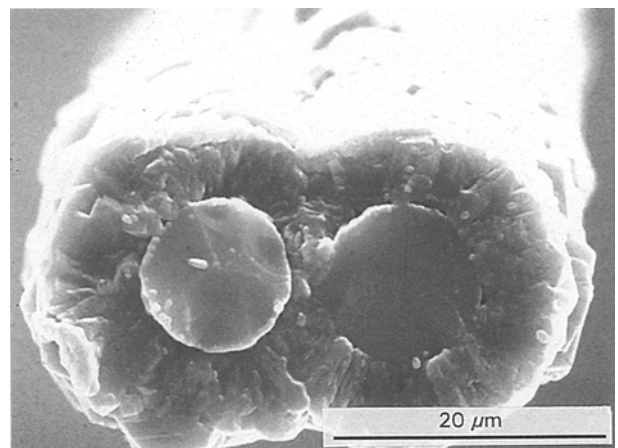


Figure 5 Example of two diamond-coated parallel Tyranno fibres after time  $t > t_c$  to form solid diamond fibre composite of cross-section  $36 \mu\text{m} \times 23 \mu\text{m}$  [12].

coating for  $t > t_c$  will increase the thickness of the sheet by  $2x_2$  (Fig. 4c) and produce a smoother surface, but the effective deposition rate in the  $X$  direction will be lower at  $R_{\text{eff}} = 2R$ . An example of a three-dimensional solid diamond/fibre section produced with two coated parallel fibres after a time  $t > t_c$  is shown in Fig. 5.

During deposition for times  $t < t_c$ , diamond can be deposited on a two-dimensional fibre array at the maximum effective rate. The arrays can be made by microresistance welding or brazing techniques or by *in situ* coating of overlapping fibre cores. An example of a diamond array made by coating a  $100 \mu\text{m}$  diameter tungsten wire is shown in Fig. 6a; note the joint formed where two wires overlap (Fig. 6b). A similar diamond fibre array made by coating a  $10 \mu\text{m}$  diameter non-conducting ceramic fibre (Tyranno Si-C-O-Ti fibre) with diamond is shown in Fig. 7. The space between the diamond fibres may be filled by infiltrating a metal [19, 20] or polymer matrix to produce diamond fibre-reinforced composites.

It follows that a planar diamond sheet could also be made by coating a planar wire spiral. The effective deposition rates of diamond normal and parallel to

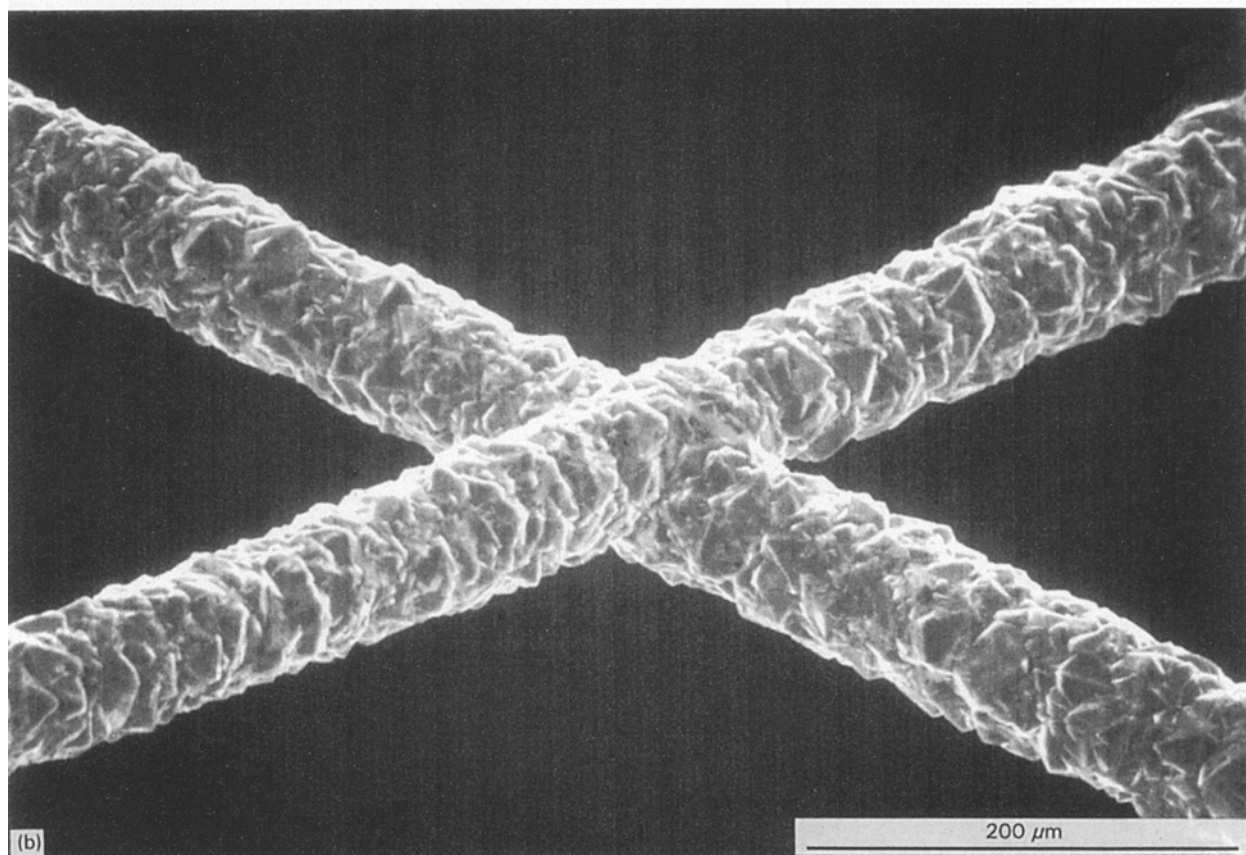
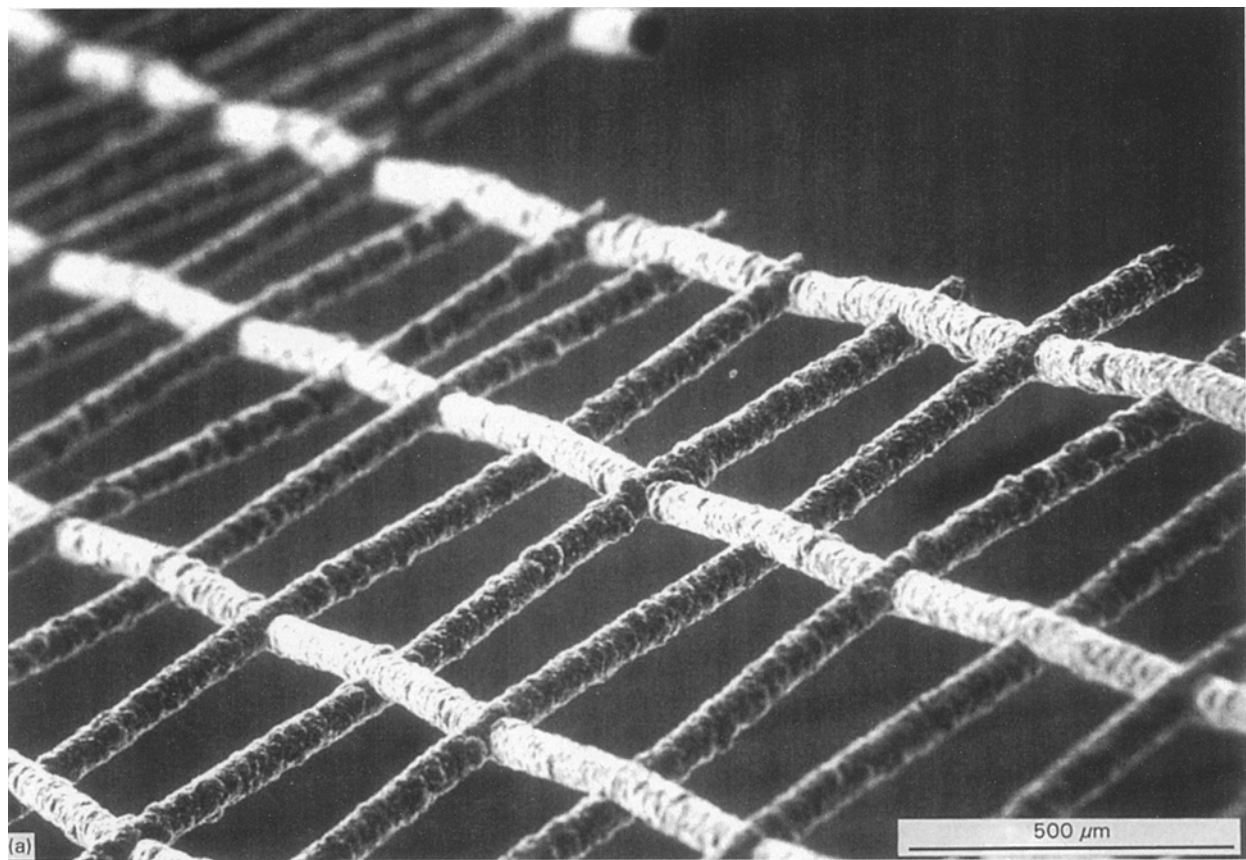


Figure 6 Scanning electron micrograph of diamond fibre arrays: (a) array of diamond fibres with tungsten wire core, and (b) detail of joint in (a) formed by diamond deposition on to overlapping tungsten wires.

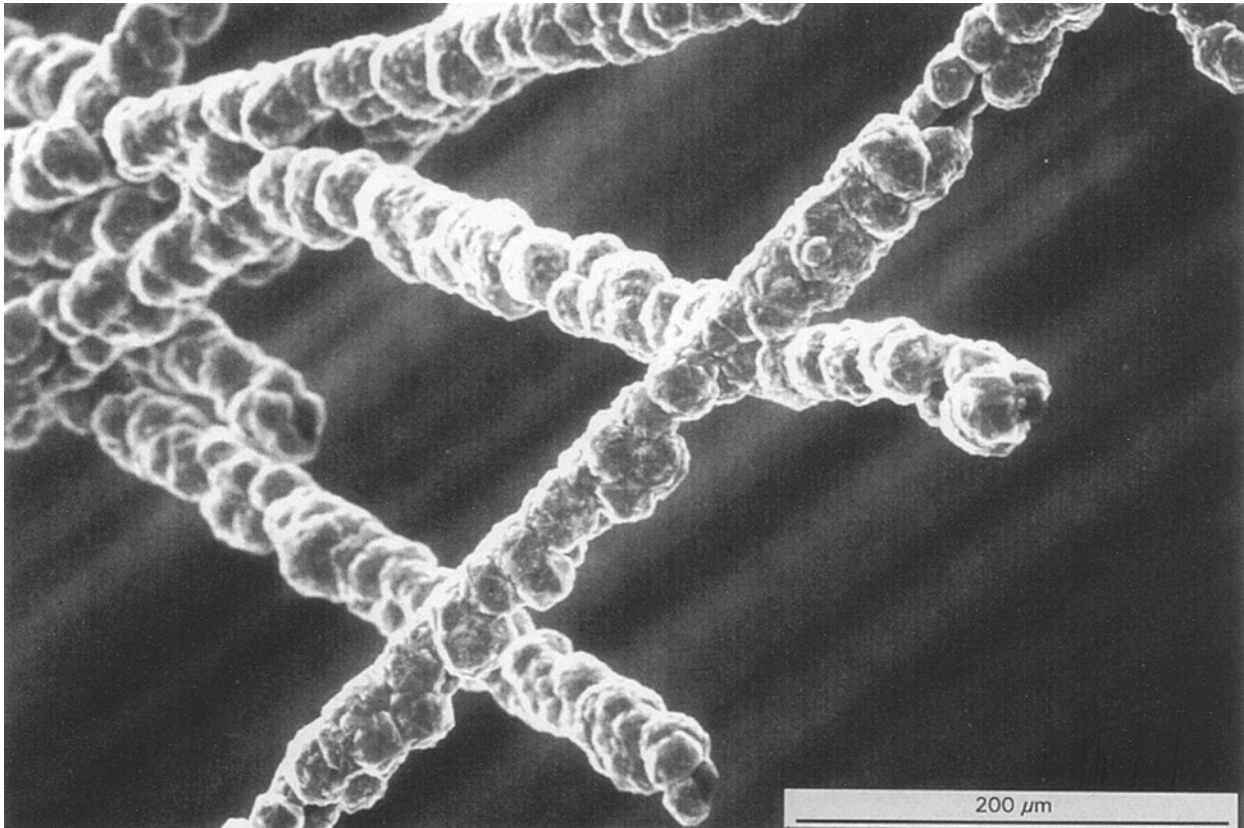


Figure 7 Scanning electron micrograph of the array of diamond fibres with Tyranno fibre cores.

a planar spiral will be  $R_{\text{eff}} = 2R$  and  $R_{\text{eff}} = 2TR$ , respectively, where  $T$  is the number of turns in the spiral.

### 5. Effective diamond deposition rate on rings

Consider diamond deposition on to a row of  $N$  circular wire rings aligned parallel along a common axis in the  $X$  direction with a distance between the rings equal to  $s$  (Fig. 8a). Let the wire diameter be  $d_1$  and the ring internal diameter be  $D$ . In this and the following deposition models, deposition will be assumed to be uniform and to occur simultaneously on all the ring surfaces. The effective diamond deposition rate, in the  $Y$  direction across the ring diameter and in the  $X$  direction along the row, will be  $R_{\text{eff}} = 4R$  and  $R_{\text{eff}} = 4NR$ , respectively. By analogy with the example of parallel wires described above, after a critical time  $t = t_c$ ,  $x_1 = s/2$ , and the space between the rings will be filled and the growing surfaces will touch as indicated in Fig. 8b. However, in this example, different shapes can be obtained depending on the values of  $D$ ,  $s$  and  $x_1$ .

When  $D > s$  and  $t = t_c$ , a hollow tube is formed (Fig. 8b). For  $t > t_c$  further deposition will occur primarily on the outside surface of the tube and increase the tube wall thickness by  $\delta x = x_2$  (Fig. 8c) and increase the tube diameter at a rate  $R_{\text{eff}} = 2x_2/t$ . As for the planar sheet above, the surface of the tube will become smoother as  $x_2$  increases.

When  $D = s$  and  $t = t_c$ , a cylindrical rod is formed as surface contact is made simultaneously between the

rings and at the centre of each ring. Isolated pores,  $P$ , are present at the centre of the rod. Further deposition will produce a larger diameter rod with the same pore size (Fig. 8d).

When  $D = 2x \ll s$ , surface contact will occur first at the centre of each ring and closed doughnut shapes will be formed. Further deposition will increase the diamond thickness on the solid doughnut shapes (Fig. 9a) until  $x_1 = s/2$  and a cylindrical rod shape is again formed with pores at  $P$  in Fig. 9b. However, note the difference in the size and shape of the pores predicted for the solid rod shapes manufactured by the two different routes (Figs 8d and 9b). It should be noted that these are idealized shapes, which are dependent on the supply of active gas species around these shapes.

### 6. Effective diamond deposition rate on helical coils

Very small diameter helical coils have been made by winding tungsten wire around wire or ceramic fibre cores (Fig. 10) and removing the cores (Fig. 11a) [21]. Diamond deposition on to the helical wire coil for a time  $t < t_c$  produces a tungsten cored diamond spring, as shown in Fig. 12a. Alternatively, when  $t = t_c$ ,  $x_1 = s/2$  and a hollow diamond tube is formed (Fig. 11b) at similar effective growth rates in the principal directions as for the row of rings considered previously (Fig. 8b). The helical wire coil is embedded in the tube wall. In a single helical coil the spacing,  $s$ , may vary along the coil length, and then for a given deposit thickness,  $x$ , regions of hollow coil and helical

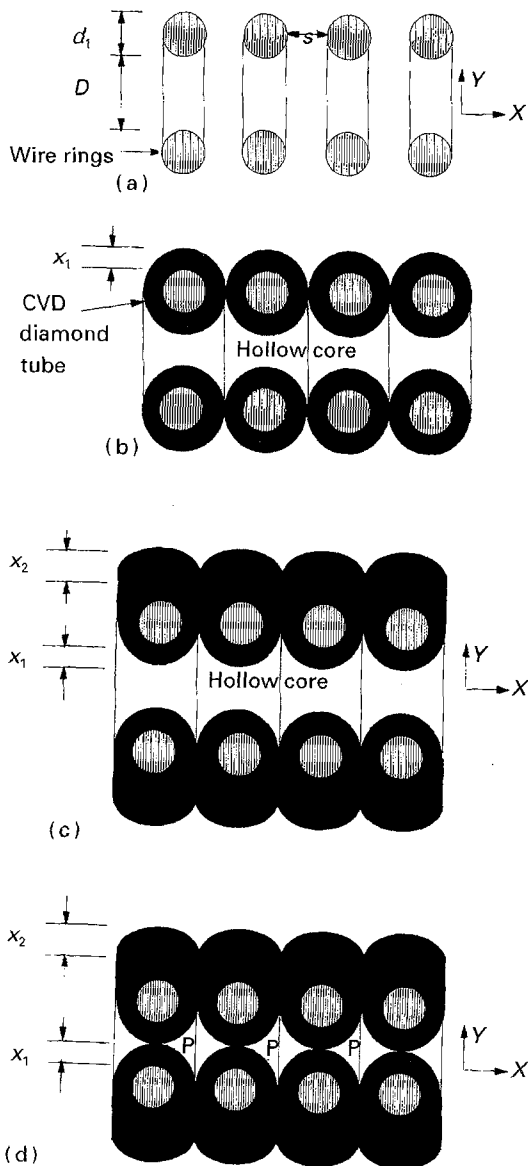


Figure 8 Schematic diagram of diamond deposition on ring cores: (a) section through row of parallel rings, (b) after diamond coating for time  $t = t_c$  to produce coating of thickness  $x_1$  and form a hollow cylinder, (c) after diamond coating for time  $t > t_c$  to produce coating of thickness  $x_1 + x_2$ , and (d) cylindrical solid bar formed with central pores at P when  $D = s$  and  $t > t_c$ .

spring may be produced, as shown in Fig. 12b. The surface and fractured end of a helical wire diamond fibre is shown in Fig. 13: note the fibre diameter is  $\sim 70 \mu\text{m}$  and the hollow core diameter is  $\sim 23 \mu\text{m}$ .

In theory, a solid rod shape might be obtained as for the parallel ring case, but with a helical pore at the centre of the rod. However, this may not be possible in practice, because deposition conditions may favour the formation of a hollow tube. Using rings or a helical coil as substrates, a thick-walled hollow diamond tube could be formed twice as fast as by conventional deposition on to a surface of a hollow cylinder [22]. If  $N$  rows of helical coils replaced the solid wires in Fig. 4, the deposition rates in the  $Y$  and  $X$  directions would be twice that for the wires, i.e.  $4R$  and  $4NR$ , respectively. Voids may be reduced in size or eliminated by selecting suitable spacings in the arrays. For example, in forming a solid cylindrical shape using

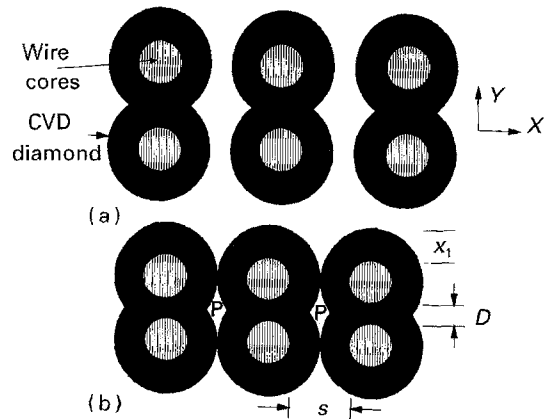


Figure 9 Schematic diagram of diamond deposition on ring cores: (a) "doughnut" shapes produced by coating rings with  $D = 2x \ll s$  and for a coating thickness  $x$ , where  $D < 2x < s$ , and (b) solid bar produced with pores at P when  $x_1 = s/2$  and  $D \ll s$ .

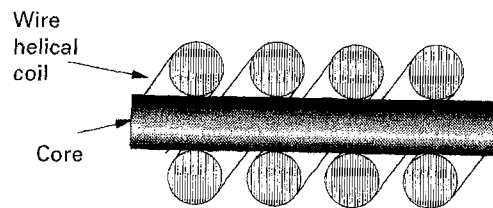


Figure 10 Production of small-diameter tungsten wire coil by winding on ceramic fibre.

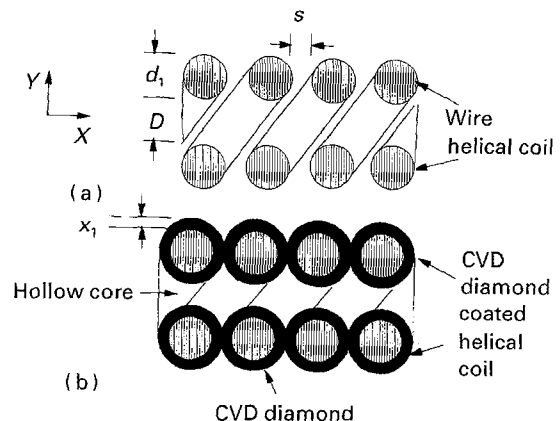


Figure 11 Schematic diagram of diamond deposition on to cylindrical coil: (a) section through coil, (b) after diamond coating for time  $t = t_c$  to produce coating of thickness  $x_1$  and a hollow cylinder.

rings, smaller voids are produced via the doughnut shape route (Fig. 9a, b) than directly via the ring route (Fig. 8d). It is possible that the size of the voids would be smaller in practice because of the ability to deposit diamond in small crevasses. A possible method of eliminating the voids is to tilt the rings to allow progressive deposition as shown in Fig. 14. These types of design changes, together with a progressive increase in the wire spacing with increase in distance from the centre of the section, will form part of the optimization

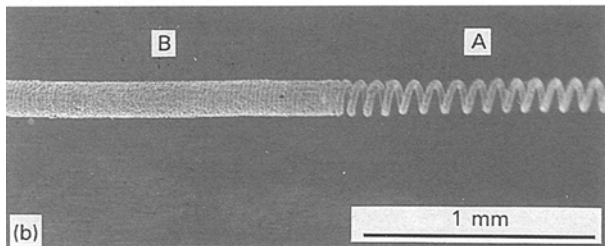
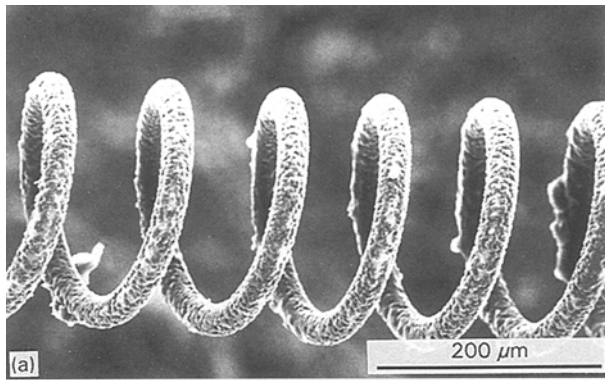


Figure 12 SEM of diamond-coated tungsten wire coils: (a) diamond-coated tungsten wire spring, and (b) coated helical coil showing spring at A where  $s > 2x_1$  and hollow cylinder at B where  $s < 2x_1$  (see text).

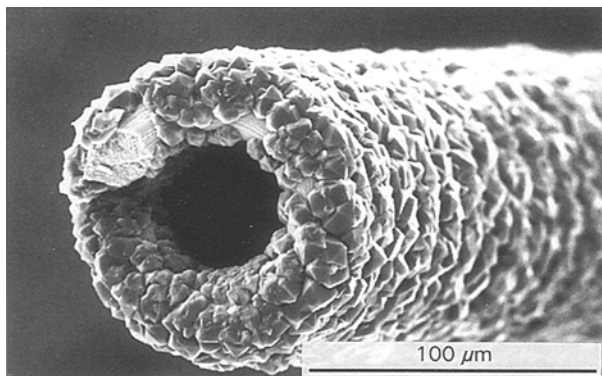


Figure 13 Scanning electron micrograph of fractured diamond-coated tungsten wire coil.

process needed to ensure maximum growth rate throughout the deposition period and maximum bulk density.

### 7. Production of short fibres and particulate diamond

High-rate deposition may be particularly suited for the manufacture of short diamond fibres or fine diamond particulates. An example of a 25 μm particle grown on a 10 μm diameter ceramic fibre is shown in Fig. 15. Consider a three-dimensional fibre array (Fig. 16a) of say  $454 \times 454 = 2 \times 10^5$  fibres each of diameter  $d_1 = 10 \mu\text{m}$  and length  $L = 50 \text{mm}$ , or an equivalent surface area in the form of a ball of separated fibre tows designed just for maximum surface area and effective deposition rate per unit volume. Assume a microwave plasma of dimensions

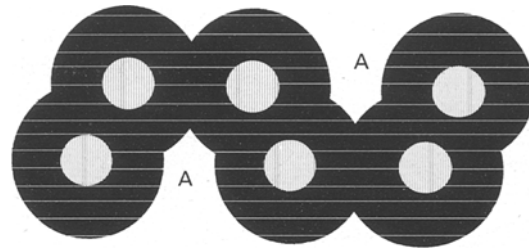


Figure 14 Schematic diagram of tilted diamond coated rings to avoid pores forming at A.

50 mm × 50 mm × 50 mm could contain such an array. If a surface diamond coating of thickness  $x = 50 \mu\text{m}$  and density of  $3.5 \text{Mg m}^{-3}$  was deposited on all these fibres (Fig. 16b), the mass of diamond would be 330 g with a volume fraction on the fibre of about 99% diamond. Assuming a typical deposition rate of  $1 \mu\text{m h}^{-1}$ , the deposition time would be 50 h, giving a CVD diamond production rate of  $330/50 = 6.6 \text{g h}^{-1}$ . This might be compared with a 1 μm thick deposit on an 8 in wafer in 1 h, corresponding to  $0.11 \text{g h}^{-1}$ . Replacing the solid fibres with helical coils would double the mass of diamond deposited per hour to  $13.2 \text{g h}^{-1}$  for  $t < t_c$ . A coated diamond fibre array could be comminuted to produce short diamond fibres or diamond particles and mixed with matrix material to form diamond-reinforced composites.

### 8. Discussion

The above observations suggest that the time required to manufacture thin or thick diamond fibre composites might be reduced substantially by coating three-dimensional arrays of straight or coiled wires or fibres. Furthermore it is worth emphasizing that these efficiency gains should be achieved with no increase in gas or power consumption.

The time to produce a thin flat diamond composite sheet of a given thickness would be reduced by a factor of 2 by using parallel or spiral wires (Figs 4b, c, 5) or by a factor of 4 by using rows of wire rings or helices (Figs 8d and 9b) instead of a single flat substrate. For example, compare the time,  $t$ , to produce a flat diamond sheet of diamond thickness  $x = 180 \mu\text{m}$  by deposition either on to a flat substrate or on to wire rings. On a flat surface at  $R = 1 \mu\text{m h}^{-1}$ ,  $t = 180 \text{h}$ . For deposition on to a row of wire rings, let the wire diameter  $d_1 = 10 \mu\text{m}$ ,  $s = D = 90 \mu\text{m}$ , and  $x_1 = 45 \mu\text{m}$  (Fig. 8a, b), to produce a 200 μm thick sheet with a diamond thickness through the regions containing the wire coils of 180 μm. The critical coating time,  $t_c$ , for the rings will be 45 h ( $R_{\text{eff}} = 4R$ ) which is four times faster than for the flat substrate. A thicker sheet may be obtained by deposition for times  $t > t_c$ , but  $R_{\text{eff}}$  at these later stages will then be reduced to  $2R$ . A smoother surface is, however, obtained (Fig. 8d). It must be emphasized that a conventional diamond sheet produced on a flat surface will have no embedded wire or ceramic core reinforcement, no pores and therefore a slightly higher volume fraction of

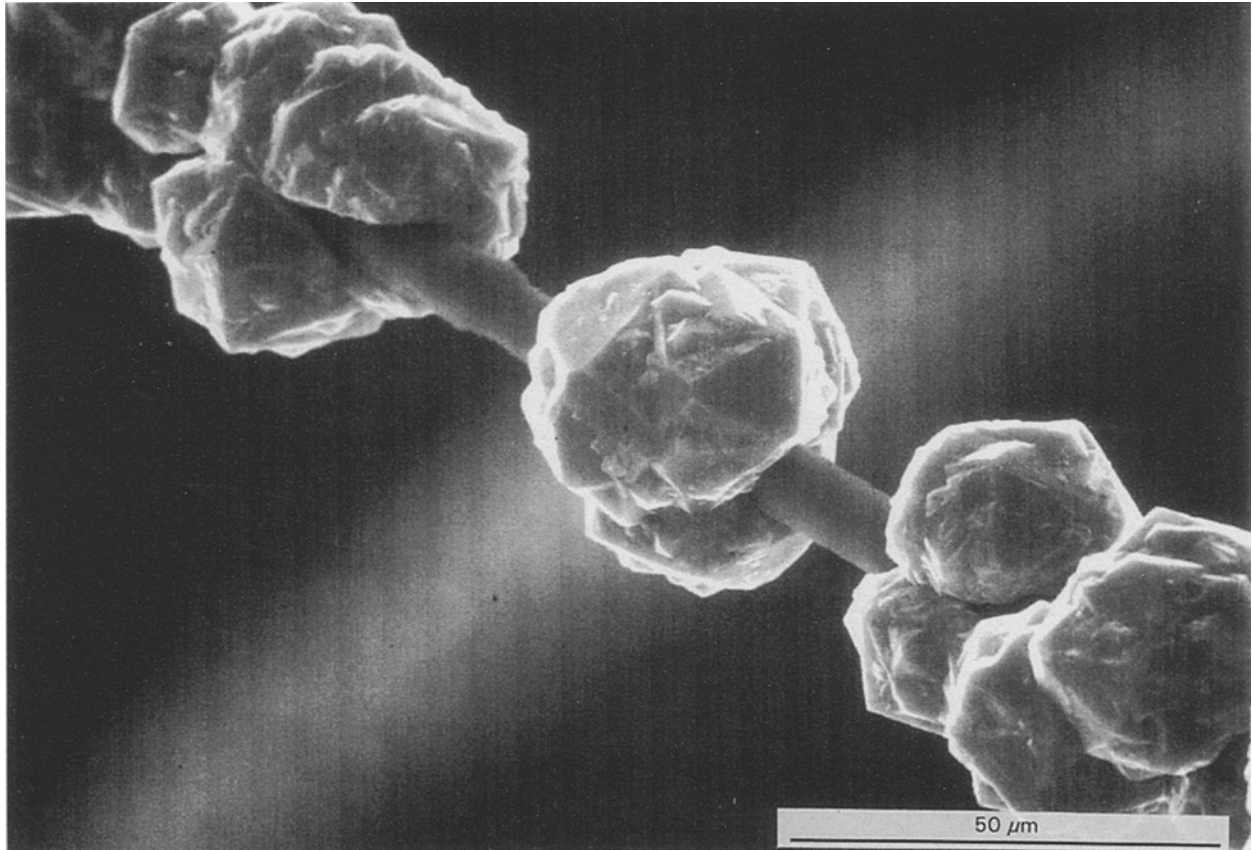


Figure 15 Particulate diamond grown on 10 µm diameter Tyranno fibre.

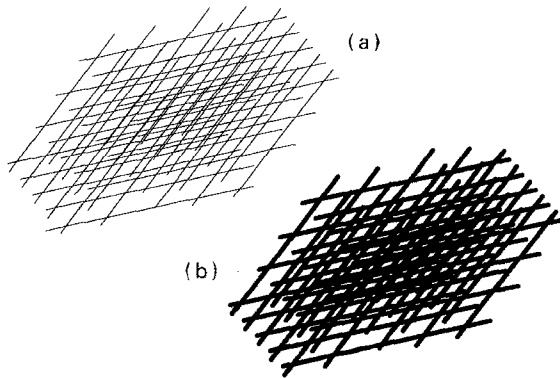


Figure 16 Schematic diagram of fibre core array: (a) before diamond coating, and (b) after diamond coating.

diamond, and will have a lower minimum thickness and a smoother surface.

Because large numbers of fibres and hence a large surface may be coated simultaneously, the effective deposition rates can be very high. Consider a hypothetical and extreme example using wires or fibres of  $d_1 = 20 \mu\text{m}$ , coated with diamond to a thickness  $x = 50 \mu\text{m}$ , to give a fibre with an outside diameter of 0.12 mm and a volume fraction of 97% diamond. A three-dimensional square array (Fig. 16) of  $100 \times 100$  fibres of say 1 m length (length limited only by the reactor size) could be coated in  $t = 50$  h at an effective rate  $10^4/50 = 200 \text{ m h}^{-1}$ . This might be compared with the deposition of 50 µm thickness of diamond on to individual 10 m length wires in 50 h at a rate of  $10/50 = 0.2 \text{ m h}^{-1}$ . This simple comparison indicates the array has the potential for coating

fibres three orders of magnitude faster than a single-fibre technique. Alternatively deposition may be continued on this array of fibres until  $t = t_c$  to manufacture a solid bar with a 12 mm  $\times$  12 mm cross-section and any length. This 12 mm thickness would consist of 10 mm thickness of diamond and would be obtained in 50 h, an effective deposition rate of  $200 \mu\text{m h}^{-1}$ . This rate is 200 times the rate for hot filament, 25 times that for combustion flame and 8 times that for the d.c. arc diamond deposition techniques on flat substrates [23]. There is no method at present proposed for making CVD diamond sections at this rate.

Hollow fibres made via the rings or helical coil route can be made in long lengths more easily than by etching [21] and are reinforced, but the internal surface is much rougher than for an etched core. When used in micro-heat exchangers this surface may promote convective heat transfer under turbulent flow conditions [24]. Free-standing tubes have been made by deposition on to one external surface of a tubular substrate [22]. A single helical coil would reduce the manufacturing time for a tube by a factor 2. A coiled coil, as used for light bulb filaments, would reduce the time by a factor of 4. There are clearly many possible design options for exploiting coils for high-rate deposition.

In designing for high effective diamond deposition rates it should be noted that increasing the effective deposition rate per unit volume by increasing the surface area per unit volume leads to more of the substrate material becoming embedded in the composite and as the growing surfaces make contact with

each other, the substrate area and the effective diamond deposition rate will decrease and porosity may arise if parts of the section become inaccessible to the active gas species.

Fibre arrays may be designed for particular shapes or contours or ease of manufacture and varying thickness and taper sections. The use of arrays should also allow fibre spacing, distribution and volume fraction to be controlled. The maximum section thickness using fibre arrays will depend partly on the CVD reactor design. The critical process stages will be the manufacture and support of the arrays during coating, and the control of temperature and gas flow rate [25] throughout the array.

To many engineers the name diamond will automatically be associated in their minds with high cost. There is, therefore, an urgent need to determine realistic estimates of current and future CVD diamond costs. In 1993 Busch and Dismukes [23] bravely attempted to assess the trends and market perspectives for CVD diamond. Their data suggested that in the long term (5–15 years) deposition rates on flat surfaces might increase to 2.57 and 3.85 g h<sup>-1</sup> for hot-filament and microwave processing, respectively, and for the higher temperature processes might increase to 13 and 15 g h<sup>-1</sup> for combustion flame and d.c. arc, respectively. It was also concluded from their cost modelling that the effect of surface area on costs was insignificant compared with the gas temperature. These conclusions may need to be reconsidered for the fibre arrays discussed in this paper, which indicate a deposition rate of ~13 g h<sup>-1</sup> might be achieved in a relatively low-cost hot-filament system using fibre coil arrays. The model also identified deposition rate and deposit thickness as having the greatest leverage on process cost. It has been shown that relatively small deposit thicknesses on very small diameter fibres can give rise to high diamond volume fractions. This combination of high effective deposition rates and low film thickness requirements suggest fibre arrays have considerable potential for cost reduction in CVD diamond processing.

It is also possible to make some cost comparisons with current commercial continuous SiC fibres [26]. An important difference between CVD of diamond and SiC is the deposition temperature. Because the CVD of diamond can be carried out at a relatively low temperature of ~900 °C compared with 1200–1300 °C for SiC [9, 10] and because electricity costs have a large effect on the deposition costs [4], this cost factor should be less for diamond. (The higher deposition temperature for SiC precludes deposition on to many metallic and non-metallic core materials suitable for diamond fibre arrays.) In the USA the reported cost of CVD diamond deposited on a flat surface at 1 µm h<sup>-1</sup> is from \$10/carat (\$50 g<sup>-1</sup>) in a 75 kW microwave reactor with 90% efficiency to \$20/carat in a hot-filament reactor [4, 5]. Taking these values and the above calculated diamond deposition rate of 6.6 g h<sup>-1</sup> for a large diamond fibre array, a cost figure for CVD diamond produced in a fibre array might be 50 × 0.15 = \$7.6 g<sup>-1</sup> (\$1.5/carat) or \$15 g<sup>-1</sup> (\$3/carat) in a microwave or hot-filament

reactor, respectively. This would be halved for arrays of helical coils. Estimates of the cost of commercial continuous SiC fibre produced in the UK and USA in 1992 were \$2.7–5.3 g<sup>-1</sup> [26]. The effective diamond deposition rate in fibre arrays and the lower diamond deposition temperature suggest that CVD diamond fibre costs could range from lower than SiC fibre to around two to three times greater than SiC fibre. Estimates also suggest that, for solid state consolidation of SiC fibre composites, the fibre costs are only about 10% of the composite cost [26]. Thus minimum processing costs are vital for low-cost composites.

## 9. Conclusion

The total mass of CVD diamond deposited per unit time per unit volume is proportional to the total substrate area per unit volume and the effective diamond deposition rate,  $R_{\text{eff}}$ , may be increased by increasing the area of substrate surface coated simultaneously. There are many design options in the coating of three-dimensional arrays of straight or coiled wires or fibres and the time to manufacture the thicker composite sections may be reduced by orders of magnitude. These efficiency gains may be achieved with no increase in gas or power consumption and could lead to substantial reductions in the cost of diamond fibre composites.

## Acknowledgements

The authors thank C. M. Ward-Close, M. Pitkethley and C. Johnston, DRA(F), for discussions on continuous fibre composites, G. Lu, C. Rego, G. Meaden and K. Mulligan for help with the experiments, and Professors J. W. Steeds and M. V. Lowson for supporting the diamond research programme. Financial support was provided by DRA(F) and EPSRC.

## References

1. P. G. PARTRIDGE, P. W. MAY and M. N. R. ASHFOLD, *Mater. Sci. Technol.* **10** (1994) 177.
2. M. N. R. ASHFOLD, P. W. MAY, C. A. REGO and N. M. EVERITT, *Chem. Soc. Rev.* **23** (1994) 21.
3. G. LU, K. J. GRAY, E. F. BORCHELT, L. K. BIGELOW and J. E. GRAEBNER, *Diamond Rel. Mater.* **2** (1993) 1064.
4. E. SEVILLANO, J. CASEY, R. GAT, S. JIN, R. S. POST and D. K. SMITH, in "Diamond Films 94", 5th European Conference On Diamond and Related Materials, Il Ciocco, Italy, September (1994) in press.
5. D. S. HOOVER, *ibid.*
6. P. W. MAY, C. A. REGO, R. M. THOMAS, M. N. R. ASHFOLD, K. N. ROSSER, P. G. PARTRIDGE and N. M. EVERITT, in "Proceedings of the 3rd International Symposium on Diamond Materials", Electrochemical Society, Honolulu (1993) p. 1036.
7. A. A. MORRISH, J. W. GLESENER, P. E. PEHRSSON, B. MARUYAMA and P. M. NATISHAN, *ibid.*, p. 834.
8. M. D. DRORY, R. J. McCLELLAND, F. W. ZOK and F. E. HEREDIA, *J. Am. Ceram. Soc.* **76** (1993) 1387.
9. A. R. BUNSELL, "Fibre reinforcements for composite materials" (Elsevier, 1988).
10. T. F. COOKE, *J. Am. Ceram. Soc.* **74** (1991) 2959.
11. A. R. BUNSELL, *Compos. Sci. Technol.* **51** (1994) 127.

12. P. W. MAY, C. A. REGO, M. N. R. ASHFOLD, K. N. ROSSER, N. M. EVERITT, P. G. PARTRIDGE, Q. S. CHIA and G. H. LU, in "Advances in new diamond science and technology" edited by S. Saito, N. Fujimori, O. Fukunaga, M. Kamo, K. Kobash and M. Yoshikama, Tokyo (1994) p. 211.
13. J. M. TING, M. L. LAKE and D. C. INGRAM, *Diamond Rel. Mater.* **2** (1993) 1069.
14. J. M. TING and M. L. LAKE, *J. Mater. Res.* **9** (1994) 636.
15. P. G. PARTRIDGE, P. W. MAY, C. REGO and M. N. R. ASHFOLD, *Mater. Sci. Technol.* **10** (1994) 505.
16. C.-M. NIU, G. TSAGAROPOULAS, J. BAGLIO, K. DURGHAT and A. WOLD, *J. Solid State Chem.* **91** (1991) 47.
17. V. P. GODBOLE and NARAYAN, *J. Mater. Res.* **7** (1992) 2785.
18. Q. S. CHIA, C. M. YOUNIS, P. G. PARTRIDGE, G. C. ALLEN, P. W. MAY and C. A. REGO, *J. Mater. Sci.* **29** (1994) 6397.
19. A. MORTENSEN and I. JIN, *Int. Mater. Rev.* **37** (1992) 101.
20. Z. ZHANG, S. LONG and H. M. FLOWER, *Compos.* **25** (1994) 380.
21. G. H. LU, P. G. PARTRIDGE and P. W. MAY, *J. Mater. Sci. Lett.* (1995) in press.
22. T. OBATA and S. MORIMOTO, *SPIE* **1146** (1989) 208.
23. J. V. BUSCH and J. P. DISMUKES, *Diamond Rel. Mater.* **3** (1994) 295.
24. P. G. PARTRIDGE, G. H. LU, J. W. STEEDS and P. W. MAY, *Diamond Rel. Mater.* (1995) 848.
25. C.-P. KLAGES, M. SATTTLER and L. SCHAFER, in "Proceedings of the 3rd International Symposium on Diamond Materials", Proceedings of the Electrochemical Society 93-17 (1993) pp. 24-33.
26. P. G. PARTRIDGE and C. M. WARD-CLOSE, *Int. Mater. Rev.* **38** (1993) 1.

*Received 20 February  
and accepted 22 March 1995*